

# Second-order Integral Fuzzy Logic Control Based Rocket Tracking Control

Iswanto <sup>1\*</sup>, Irfan Ahmad <sup>2</sup>

<sup>1</sup>Department of Electrical Engineering, Universitas Muhammadiyah Yogyakarta, Yogyakarta, Indonesia

<sup>2</sup>Department of Electrical Engineering, Khurasan university, Afghanistan

Email: <sup>1</sup> iswanto\_te@umy.ac.id, <sup>2</sup> irfan.ahmed.mcse@gmail.com

\*Corresponding Author

**Abstract**— Fuzzy logic is a logic with a degree of vulnerability ranging from 0 to 1. Fuzzy logic is used to convert a quantity into language. It is used as a control system because it is a versatile and simple control process that does not require complex mathematical models. The paper aimed to present a fuzzy control system implemented in a rocket tracking control system as the controller because it could work well on non-linear systems and offered convenience in program design. The fuzzy control system worked to keep the rocket on track and travel at a fixed speed. The signal from the fuzzy logic control system served to control the rocket thrust. However, the process of the fuzzy logic control system is slow and time-consuming, not proper for the one that required rapid control, such as rockets, and is not applicable for tracking ramp and parabolic signals. The fuzzy logic, therefore, was modified by adding second-order integral control. The proposed algorithm showed that, by adding second-order integral control, the rocket glided 12.78m at 12 seconds with a steady-state error of 0.78 according to the setpoint of ramp path 12 m; 10.68m at 10 seconds with a steady-state error of 0.68 according to the setpoint of ramp path 10m; and 4.689m at 4 seconds with a steady-state error of 0.689 according to the setpoint of ramp path 4m. In accordance with the parabolic path, the rocket glided 15.47m at the 4th minute with 0 steady-state error.

**Keywords**— *second-order integral control; FLC; Ramp; Parabolic*

## I. INTRODUCTION

Fuzzy logic is an improvement over Boolean logic, which has something in common with partial truth. Fuzzy logic can be useful for determining a value between 0 and 1. Fuzzy logic is not the same as classical logic. Fuzzy logic deals with inequality, uncertainty, and partial truth. It is this reason that makes it easier to implement fuzzy logic control for linear models compared to other conventional control techniques. Fuzzy logic has been widely applied in the automatic and industrial control field, including image processing, motor, robot, and aircraft controls. It can simulate human experience about the best way to control the system without requiring accurate model equations and handle problems in a system. It also offers a solution for uncertainty by mimicking the human experience in the form of rules to control a system automatically.

Fuzzy logic methods have been researched, such as optimized aco algorithm fuzzy pid controller for load frequency control in multi-area interconnected power systems by G. Chen. [1]. The UUV track tracking control based on backstepping shear mode with fuzzy diverting

reinforcement in the dive field by Yang [2]. Fuzzy based super-twisting shear mode stabilization control for driven rotary reverse pendulum system by Nguyen [3]. experimental investigation of the fuzzy adaptive global shift mode control of a single-phase shunt active power filter by Hou [4] and fuzzy reinforcement scheduling and feed-forward control for the chlorination process of drinking water treatment plants (DWTP) investigated by Gamiz [5].

You investigated adaptive fuzzy control for a nonlinear state limited system with unknown input delay and control coefficient [6]. Tang studied a control strategy based on the fuzzy Takagi-Sugeno model for variable stiffness and variable damping suspension [7]. Yang examined Fuzzy PI based on EKF sensor speed control, optimal control of power from direct drive power system [8]. Oliveira designed online neuro-fuzzy controller robust stability [9]. Tran researched adaptive fuzzy control method for single tilt tricopter [10].

Extended Fuzzy Adaptive Event Trigger Compensation Control for Unspecified Nonlinear Systems with Input Hysteresis was investigated by Huang [11]. High Order Shift Mode Backward Step Control for Classes of Unknown Pure Feedback Nonlinear Systems was investigated by Liu [12]. Fuzzy Type Fast Terminal Shift Mode Controller for Pilot Solenoid Valve Pressure Control in Automatic Transmission was investigated by Fan [13]. Shear Impedance Mode Control with Adaptive Fuzzy Compensation for Robot Environment Interaction was investigated by Hu [14]. Actor-Critic Reinforcement Learning Control from a Dynamic Non-Strict Feedback System Nonaffine was investigated by Bu [15].

Sadeq used the optimal control strategy to maximize electric vehicle hybrid energy storage system performance considering topographical information [16]. Rezk designed and implemented new MPPT control method based on fuzzy logic for photovoltaic applications [17]. Liu investigated adaptive fuzzy control for generalized hindmarsh-rose neuron [18]. Xuw studied fuzzy controller for autonomous vehicles based on coarse sets [19]. Wu examined fuzzy cmac based adaptive scale force control of exoskeletons weight support [20].

Autonomous mobile target tracking for fuzzy-pi based UAV quadcopter was investigated by Rabah [21]. direct current motor speed control using ANFIS-based hybrid



configuration controller P-I-D was investigated by Guo [22]. Multi-stage shift control scheme for electrical mechanical transmission: design and experiment was researched by Bao [23]. Static Output Feedback Control for Fuzzy Systems with stochastic fading channels and actuator errors was investigated by Chen [24]. Input-to-state stabilization of uncertain parabolic PDE using observer-based fuzzy control was investigated by Kang [25].

Liu investigated allocation of strong power for femtocell networks using fuzzy estimation of dynamic channel status [26]. X. Liu studied fuzzy-set theory-based optimal robust design for permanent magnet linear motor position tracking control [27]. Wu researched cross-domain grain data usage control services for industrial wireless sensor networks [28]. Zhao studied fuzzy logic-based coordinated control of a battery energy storage system and a distributed generator for microgrids [29]. Kuo examined the development of an automatic emotional musical accompaniment system with fuzzy logic and an adaptive partitioning evolutionary genetic algorithm [30].

Fuzzy logic control algorithms have been widely used for robot control and other equipment control. Tracking control has been applied to the Quadrotor based on the research that has been mentioned. The authors proposed a rocket tracking control method using fuzzy artificial intelligence control algorithms to optimizes the member set error for a faster rise time.

## II. ROCKET MODELING

The electric ducted fan (EDF) rocket is a flying object in the shape of a bullet using a shrouded electric motor as the propulsion shown in Figure 1. Four EDF motors were used as the rocket thrusts. The rocket was controlled autonomously to determine the rocket's attitude towards Earth's gravity and Earth's magnetism. The control system was required to control the four rocket propulsion engines. The EDF rocket system was a non-linear system with rotors at each end, resembling a quadrotor [31] which was modeled using Euler angles to have six degrees of freedom defined by twelve states.

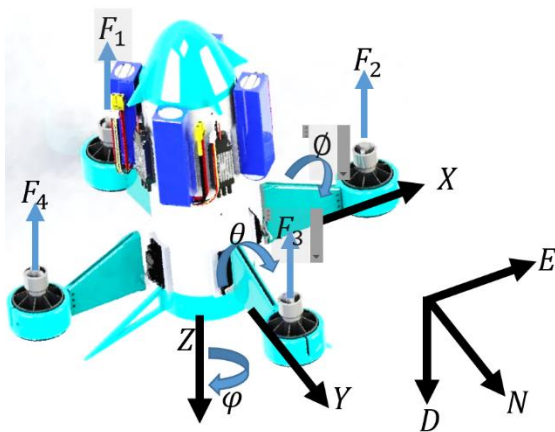


Fig. 1. Missile modeling with Euler angles

Model representation of the rocket system  $x = [x \ y \ z \ \phi \ \theta \ \varphi \ \dot{x} \ \dot{y} \ \dot{z} \ \dot{\phi} \ \dot{\theta} \ \dot{\varphi}]^T$  of all 12 equations does not linear can be formulated as

$$\dot{x}_1 = \dot{x} = x_7 \quad (1)$$

$$\dot{x}_2 = \dot{y} = x_8 \quad (2)$$

$$\dot{x}_3 = \dot{z} = x_9 \quad (3)$$

$$\dot{x}_4 = \dot{\phi} = x_{10} + s_{x_4} t_{x_5} x_{11} + c_{x_4} t_{x_5} x_{12} \quad (4)$$

$$\dot{x}_5 = \dot{\theta} = c_{x_4} x_{11} + s_{x_4} x_{12} \quad (5)$$

$$\dot{x}_6 = \dot{\varphi} = \frac{s_{x_4}}{c_{x_5}} x_{11} + \frac{c_{x_4}}{c_{x_5}} x_{12} \quad (6)$$

$$\dot{x}_7 = \dot{\dot{x}} = -\frac{1}{m} T (c_{x_4} s_{x_5} c_{x_6} + s_{x_4} s_{x_6}) \quad (7)$$

$$\dot{x}_8 = \dot{\dot{y}} = -\frac{1}{m} T (c_{x_4} s_{x_5} s_{x_6} - s_{x_4} c_{x_6}) \quad (8)$$

$$\dot{x}_9 = \dot{\dot{z}} = g - \frac{1}{m} T (c_{x_4} c_{x_5}) \quad (9)$$

$$\dot{x}_{10} = \dot{\ddot{\phi}} = \frac{\tau_x}{I_x} - \frac{I_z - I_y}{I_x} x_{11} x_{12} \quad (10)$$

$$\dot{x}_{11} = \dot{\ddot{\theta}} = \frac{\tau_y}{I_y} - \frac{I_x - I_z}{I_y} x_{10} x_{12} \quad (11)$$

$$\dot{x}_{12} = \dot{\ddot{\varphi}} = \frac{\tau_z}{I_z} - \frac{I_y - I_x}{I_z} x_{10} x_{11} \quad (12)$$

where  $c_\theta = \cos\theta$ ,  $c_\varphi = \cos\varphi$ ,  $c_\phi = \cos\phi$ ,  $s_\theta = \sin\theta$ ,  $s_\varphi = \sin\varphi$ , and  $s_\phi = \sin\phi$ .

## III. CONTROL STRATEGY

This paper presents rocket tracking control using a modified fuzzy algorithm, while the rocket-controlled system is non-linear. A method is needed to linearize the system, to facilitate controls. The non-linear model of the rocket was then linearized at the equilibrium point so that the system can be processed in a linear model. In linearizing, we must find the equilibrium point of the rocket, so that it can be written as  $0 = f(X(\alpha, \beta, \gamma, \delta))$ . So that the 12 non-linear equations can be written,

$$\dot{x}_1 = \dot{x} = x_7 = 0 \quad (13)$$

$$\dot{x}_2 = \dot{y} = x_8 = 0 \quad (14)$$

$$\dot{x}_3 = \dot{z} = x_9 = 0 \quad (15)$$

$$\dot{x}_4 = \dot{\phi} = x_{10} + s_{x_4} t_{x_5} x_{11} + c_{x_4} t_{x_5} x_{12} = 0 \quad (16)$$

$$\dot{x}_5 = \dot{\theta} = c_{x_4} x_{11} + s_{x_4} x_{12} = 0 \quad (17)$$

$$\dot{x}_6 = \dot{\phi} = \frac{s_{x_4}}{c_{x_5}} x_{11} + \frac{c_{x_4}}{c_{x_5}} x_{12} = 0 \quad (18)$$

$$\dot{x}_7 = \dot{x} = -\frac{1}{m} T(c_{x_4} s_{x_5} c_{x_6} + s_{x_4} s_{x_6}) = 0 \quad (19)$$

$$\dot{x}_8 = \dot{y} = -\frac{1}{m} T(c_{x_4} s_{x_5} s_{x_6} - s_{x_4} c_{x_6}) = 0 \quad (20)$$

$$\dot{x}_9 = \dot{z} = g - \frac{1}{m} T(c_{x_4} c_{x_5}) = 0 \quad (21)$$

$$\dot{x}_{10} = \dot{p} = \frac{\tau_x}{I_x} - \frac{I_z - I_y}{I_x} x_{11} x_{12} = 0 \quad (22)$$

$$\dot{x}_{11} = \dot{q} = \frac{\tau_y}{I_y} - \frac{I_x - I_z}{I_y} x_{10} x_{12} = 0 \quad (23)$$

$$\dot{x}_{12} = \dot{r} = \frac{\tau_z}{I_z} - \frac{I_y - I_x}{I_z} x_{10} x_{11} = 0 \quad (24)$$

If it is assumed that the equilibrium point is located at several positions in the Cartesian coordinates (x, y, z) and at several positions of the yaw angle defined as  $x_1 = \alpha$ ,  $x_2 = \beta$ ,  $x_3 = \gamma$ , and  $x_6 = \delta$ , then the value of all state equations at this equilibrium point is,  $X(\alpha, \beta, \gamma, \delta)$ , so it can be written as,  $x_1 = \alpha$ ,  $x_2 = \beta$ ,  $x_3 = \gamma$ ,  $x_4 = 0$ ,  $x_5 = 0$ ,  $x_6 = \delta$ ,  $x_7 = 0$ ,  $x_8 = 0$ ,  $x_9 = 0$ ,  $x_{10} = 0$ ,  $x_{11} = 0$ , and  $x_{12} = 0$

The following is the representation of the state equation and the system output.

$$\begin{aligned} \dot{x} &= Ax + Bu, \\ y &= Cx + Du, \end{aligned} \quad (25)$$

where matrices  $A$  and  $B$  are obtained using the Jacobi linearization method. Matrices  $A$  and  $B$  are derived partially on the nonlinear model.

$$A = \begin{bmatrix} \frac{\partial f_1}{\partial x_1} |X(\alpha, \beta, \gamma, \delta) & \dots & \frac{\partial f_1}{\partial x_{12}} |X(\alpha, \beta, \gamma, \delta) \\ \vdots & \ddots & \vdots \\ \frac{\partial f_{12}}{\partial x_1} |X(\alpha, \beta, \gamma, \delta) & \dots & \frac{\partial f_{12}}{\partial x_{12}} |X(\alpha, \beta, \gamma, \delta) \end{bmatrix}, \quad (26)$$

$$B = \begin{bmatrix} \frac{\partial f_1}{\partial u_1} |X(\alpha, \beta, \gamma, \delta) & \dots & \frac{\partial f_1}{\partial u_4} |X(\alpha, \beta, \gamma, \delta) \\ \vdots & \ddots & \vdots \\ \frac{\partial f_{12}}{\partial u_1} |X(\alpha, \beta, \gamma, \delta) & \dots & \frac{\partial f_{12}}{\partial u_4} |X(\alpha, \beta, \gamma, \delta) \end{bmatrix}. \quad (27)$$

Then, we get the  $A$  and  $B$  matrices

$$A = \begin{bmatrix} O_{(6 \times 6)} & I_{(6 \times 6)} \\ O_{(2 \times 3)} & N_{(2 \times 2)} & O_{(2 \times 1)} & I_{(6 \times 6)} \\ O_{(4 \times 6)} & & & \end{bmatrix}. \quad (28)$$

$$B_{(12 \times 4)} = \begin{bmatrix} O_{(8 \times 4)} \\ M_{(4 \times 4)} \end{bmatrix}. \quad (29)$$

where  $O$  is the zero matrix and  $I$  is the identity matrix. Meanwhile,  $N$  and  $M$  can be defined as:

$$N_{(2 \times 2)} = \begin{bmatrix} 0 & -g \\ g & 0 \end{bmatrix}. \quad (30)$$

$$M_{(4 \times 4)} = \begin{bmatrix} -\frac{b}{m} & -\frac{b}{m} & -\frac{b}{m} & -\frac{b}{m} \\ 0 & -\frac{db}{I_x} & 0 & \frac{db}{I_x} \\ \frac{db}{I_y} & 0 & -\frac{db}{I_y} & 0 \\ \frac{k}{I_z} & -\frac{k}{I_z} & \frac{k}{I_z} & -\frac{k}{I_z} \end{bmatrix}. \quad (31)$$

The output of the quadrotor model can be defined by the  $y$  vector as follows:

$$y = [x \quad y \quad z \quad \varphi]. \quad (32)$$

so that the matrix  $C$  and  $D$  can be written as

$$C_{4 \times 12} = \begin{bmatrix} I_{(3 \times 3)} & O_{(3 \times 9)} \\ O_{(1 \times 3)} & L_{(1 \times 9)} \end{bmatrix}. \quad (33)$$

$$D = 0. \quad (34)$$

with

$$L_{(1 \times 9)} = [1 \quad 1 \quad 1 \quad 0 \quad 0 \quad 1 \quad 0 \quad 0 \quad 0]. \quad (35)$$

Thus, the rocket linearization model is

$$\dot{x} = A_{12 \times 12} x + B_{12 \times 4} u, \quad (36)$$

$$y = C_{4 \times 12} x. \quad (37)$$

With linearization using equilibrium, all state equations except  $x$ ,  $y$ ,  $z$ , and yaw were assumed to have minute values. Then, the inputs for all four motors were assumed to have the same speed so that the MIMO system could be simplified into a SISO system by using the rate of change in altitude and altitude. The equation is formulated as follows [32].

$$\dot{x}_3 = \dot{z} = x_9 \quad (38)$$

$$\dot{x}_9 = \dot{z} = g - \frac{1}{m} T(c_{x_4} c_{x_5}). \quad (39)$$

Then, the equation of the state of the quadrotor altitude system can be defined as follows

$$\begin{aligned} \dot{x}_g &= A_g x + B_g u, \\ y &= C_g x. \end{aligned} \quad (40)$$

where the value of  $\dot{x}_\theta = [\dot{x}_3 \ \dot{x}_9]^T$ ,  $x = [x_3 \ x_9]$ ,  $A_\theta = \begin{bmatrix} 0 & 1 \\ 0 & 0 \end{bmatrix}$ ,  $B_\theta = \begin{bmatrix} 0 \\ -4v \end{bmatrix}$ , and  $C_\theta = [1 \ 0]$  and the transfer function of  $z$  can be defined by the following equation.

$$G_{(s)} = \frac{-4v}{s^2}. \tag{41}$$

This paper presents the rocket tracking control for tracking ramp and parabolic input signals. A block diagram of rocket tracking control was designed using equation 41. Figure 2 illustrates the first design. The figure shows that the artificial intelligence control is the FLC control modified into proportional control and derivative control [32]. The output from the fuzzy control was added up and then entered into the throttle.

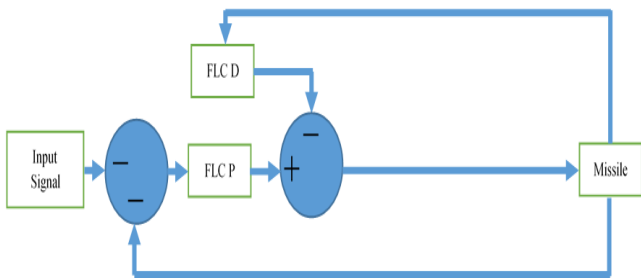


Fig. 2. Modified FLC control block diagram

Figure 3 illustrates the designs for the two rocket tracking control systems. The modified FLC is combined with the integral FLC, which is used for rocket tracking control, as seen in the figure. The integral FLC, the modified FLC summing, then enters into the throttle.

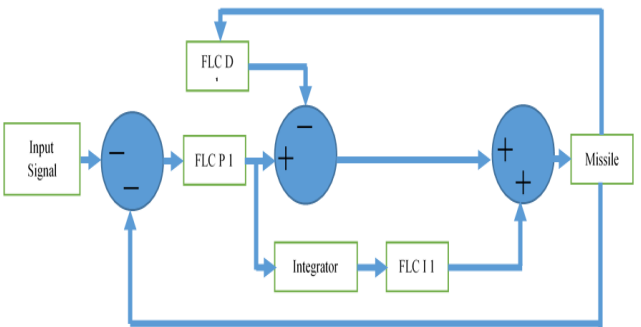


Fig. 3. Integral FLC block diagram

Figure 4 illustrates the third design of the rocket tracking control. The modified FLC is coupled with the second-order integral FLC for rocket tracking control. The output of the modified FLC adds up to the integral FLC 1 and the integral FLC 2, then enters the throttle.

The design of the four-rocket tracking control is illustrated in Figure 5. The modified FLC control was combined with the second-order integral fuzzy logic controller and the proportional control for rocket tracking control.

The figure shows that there is one proportional controller, two integrator controllers, and four fuzzy logic algorithm controls, namely proportional fuzzy logic controller 1 (FLC P 1), fuzzy logic controller derivative 1 (FLC D 1), the

integral fuzzy logic controller 1 (FLC I 1), and integral fuzzy logic controller 2 (FLC I 2). It is seen in the figure that the fuzzy logic controller has an input and an output.

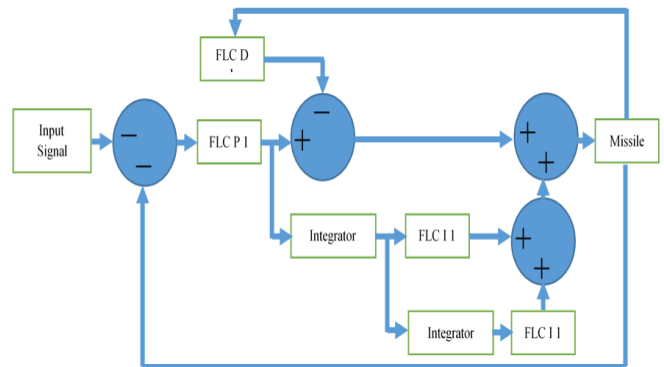


Fig. 4. Block diagram of the second-order integral FLC

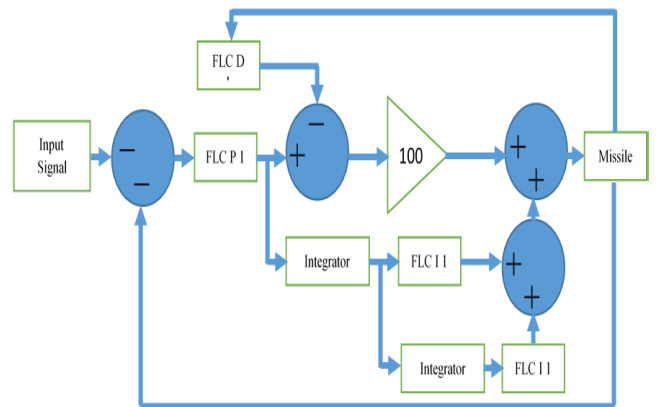


Fig. 5. Block diagram of the second-order integral FLC

The rocket tracking control proposed in this study used a fuzzy logic controller algorithm with a 3x3 rule base. The design of the fuzzy rule base used a lookup table 9 rules to determine decisions presented in Table 1. The table presents two inputs, namely input 1 and input 2. Input 2 has the same value as 1. The input and output have three membership functions, namely NS, Z, and PS for the input and POSITIVE, ZERO, and NEGATIVE for the output.

TABLE I. BASIC RULES OF FUZZY LOGIC CONTROLLERS

		INPUT 1		
		NS	Z	PS
INPUT 2	1	POSITIVE	POSITIVE	NOL
	1	POSITIVE	NOL	NEGATIVE
	1	NOL	NEGATIVE	NEGATIVE

Figure 6 illustrates the proportional fuzzy logic controller input variables, where the range of the speaker inputs NS, Z, and PS are [-1 1]. The fuzzy set for the three membership functions of NS, Z, and PS are [-2.727 -1.818 -0.9091 0], [-0.9303 -0.02116 0.8879], [0 0.9091 1.818 2.727], respectively.

Figure 7 shows the proportional fuzzy logic controller output variables, with NEGATIVE, ZERO, and POSITIVE as the speaker inputs. The fuzzy sets for NEGATIVE, ZERO, AND POSITIVE membership functions are [-363.6 -181.8 -90.9 0], [-90.9 0 90.9], and [0 90.9 181.8 272.8], respectively.

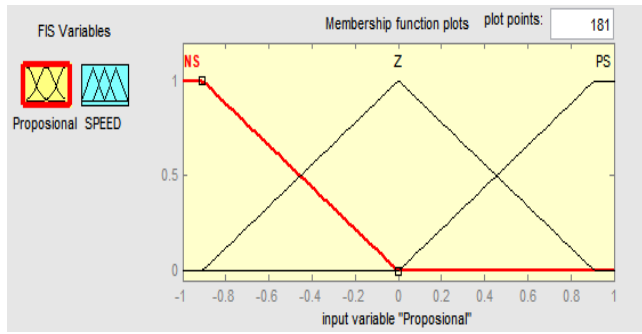


Fig. 6. Designing the FLCP input variable proposional

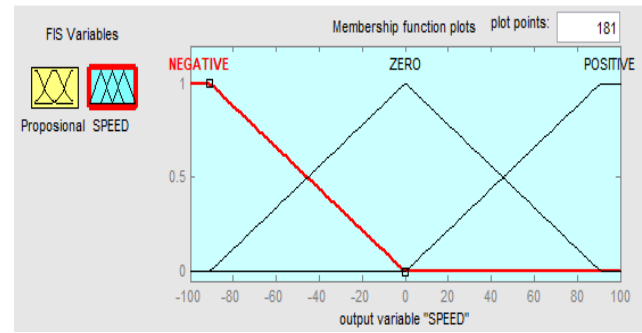


Fig. 7. Design of FLCP variable speed output

Figure 8 illustrates the derivative fuzzy logic controller input variables, where the range of the speaker inputs NS, Z, and PS are [-0.5 0.5]. The fuzzy set for the three membership functions of NS, Z, and PS are [-1.2 -0.8 -0.4 0], [-0.4 0 0.4], and [0 0.4 0.8 1.2], respectively.

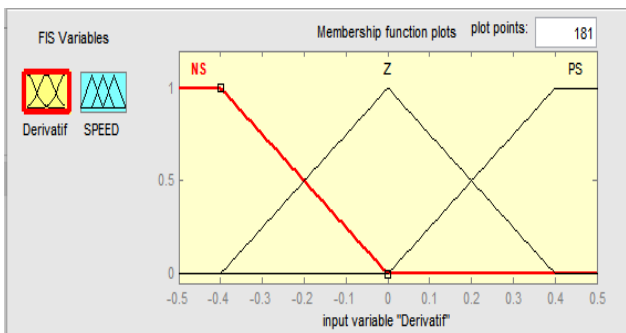


Fig. 8. Designing FLCD variable derivative input

The output variables of the fuzzy logic controller are shown in Figure 9, where the speaker's inputs are NEGATIVE, ZERO, and POSITIVE. The fuzzy set for NEGATIVE, ZERO, AND POSITIVE membership functions is [-363.6 -181.8 -90.95 0], [-90.95 0 90.95], and [0 90.95 181.8 272.8], respectively.

Figure 10 illustrates the integral 1 fuzzy logic controller input variables, where the range of the speaker inputs NS, Z, and PS are [-0.5 0.5]. The fuzzy set for the three membership functions of NS, Z, and PS are [-1.2 -0.8 -0.4 0], [-0.4 0 0.4], and [0 0.4 0.8 1.2], respectively.

Figure 11 shows the output variables of a derivative fuzzy logic controller, where the speaker's inputs are NEGATIVE, ZERO, and POSITIVE. The fuzzy set for NEGATIVE, ZERO, AND POSITIVE membership functions is [-1819 -

908.6 -454.6 0], [-454.6 0 454.6], and 0 454.6 908.6 1364], respectively.

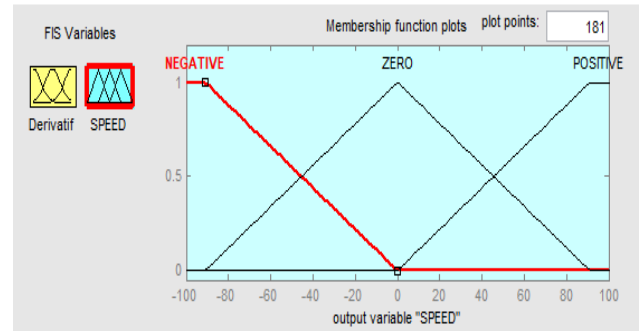


Fig. 9. FLCD variable speed input design

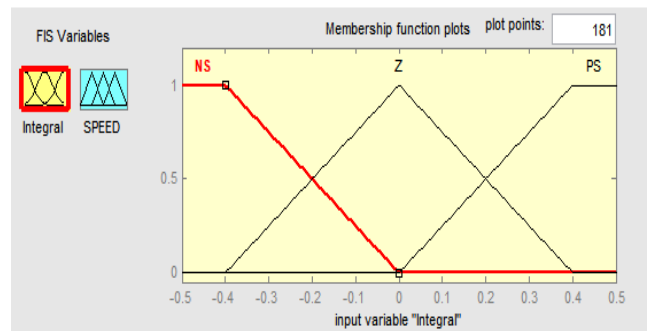


Fig. 10. The design of the FLCII integral variable input

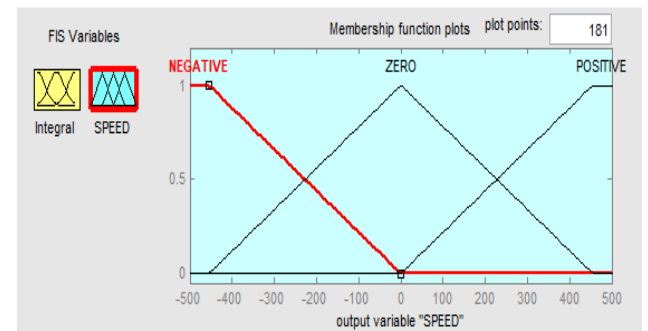


Fig. 11. Design of FLCII variable speed input

The design of the integral 2 fuzzy logic controller variable input is shown in Figure 12. The speakers for the NS, Z, and PS input ranges are [-0.5 0.5]. It can be seen that there are three membership functions, namely NS, Z, and PS. The three membership functions each has a fuzzy set, namely NS with domain [-1.2 -0.8 -0.4 0], Z with domain [-0.4 0 0.4], and PS with domain [0 0.4 0.8 1.2].

The design of the derivative fuzzy logic controller variable output is shown in Figure 13, which shows that the NEGATIVE, ZERO, and POSITIVE input speaker universes have a range value of [-500 500]. From the figure, it can be seen that there are three membership functions, namely NEGATIVE, ZERO, and POSITIVE. The three membership functions each have a fuzzy set, namely NEGATIVE having a domain [-1819 -908.6 -454.6 0], NOL having a domain [-454.6 0 454.6], and POSITIVE having a domain [0 454.6 908.6 1364].

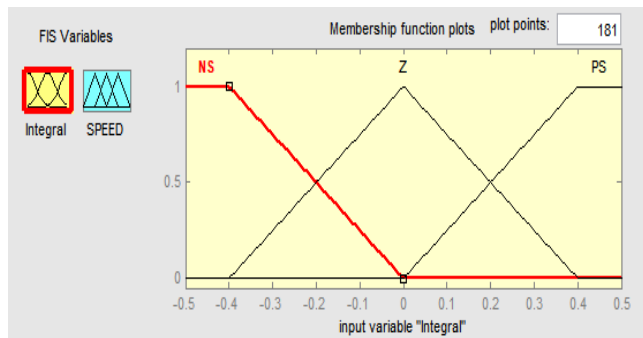


Fig. 12. The design of the FLC12 integral variable input

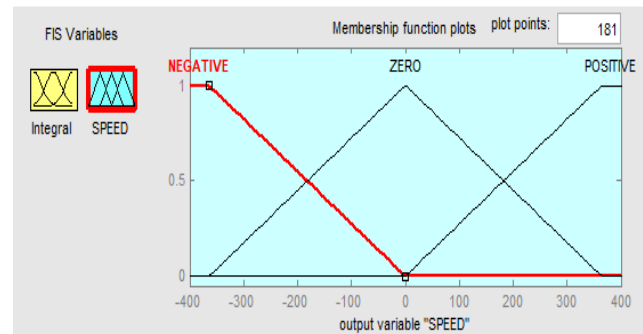


Fig. 13. Design of FLC12 variable speed output

IV. RESULTS AND ANALYSIS

In this paper, the fuzzy logic control algorithm used for rocket tracking control was simulated using Corke's [31] simulator with specifications presented in Table 2. The rocket mass was 4 kg, the constant thrust  $1.2953 \times 10^{-5}$  Kg.m, and the drag constant  $1.0368 \times 10^{-7}$  Kg.m. It was tested at the gravitational acceleration of 9.8m/s<sup>2</sup>. The parameters in the simulator were adjusted, such as setting the initial position of the rocket in the XY (-1,0) position, to simulate tracking rocket control.

A. Observation of the rocket without disturbance

The experiments were carried out using Iswanto's modified fuzzy control without wind disturbances [32]. The rocket was placed on the z-axis at 0.15 m, and the x and y axes are in the initial position (0,0). In the first experiment, the Rocket was set to track the ramp signal without interference at the z-axis shown in Figure 14.

TABLE II. MODEL ROCKET PARAMETERS

Parameter	Value	Unit	Remark
G	9.81	m/s <sup>2</sup>	Gravitational speed
M	4.34	Kg	Rocket mass
B	$1.2953 \times 10^{-5}$	Kg.m	Thrust constant
K	$1.0368 \times 10^{-7}$	Kg.m	Friction Constant
I <sub>x</sub>	0.082	Kg.m <sup>2</sup>	Moment Inertia of x-axis
I <sub>y</sub>	0.0845	Kg.m <sup>2</sup>	Moment Inertia of y-axis
I <sub>z</sub>	0.1377	Kg.m <sup>2</sup>	Moment Inertia of z-axis

In all figure, three colors were used for the graph, namely black, cyan, green, red, blue and magenta as shown in figure 13. Six graphs in the figure were the setpoint represented in

the black curve, the balance in the cyan curve, pvz0 in the green curve, pvz1 in the red curve, pvz2 in the blue curve, and pvz3 in the magenta curve.

Four curves were the ez0 curve shown in green, the ez1 curve in red, the ez2 curve in blue, and ez3 curve in a magenta. The FLC used for rocket tracking control was represented by the pvz0 curve, the integral FLC by the pvz1 curve, the second-order integral FLC with proportional control by the pvz2 curve, and the PD by the pvz3 curve.

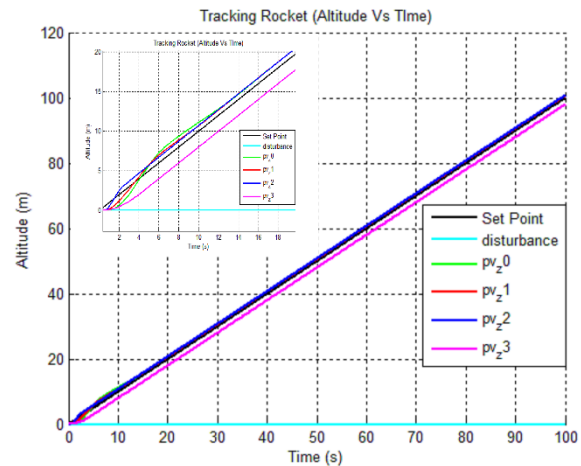


Fig. 14. Design of tracking rocket ramp

The measurement result of the rocket altitude in Figure 14 is as follow. When it glided for 2 seconds with a setpoint value of 2 meters, the altitude of the rocket measured by PD on pvz3 was 0.4675, by the second-order integral fuzzy on pvz2 was 1.466, by the integral fuzzy logic on pvz1 was 1.178, and by the fuzzy logic controller on pvz0 was 0.6598. When it glided for 4 seconds with a setpoint value of 4 meters, the altitude of the rocket measured by PD on the pvz3 graph was 2014, by the second-order integral fuzzy logic on pvz2 was 4.279, by the integral fuzzy on pvz1 was 4.236, and by the fuzzy logic controller on pvz0 was of 3.828.

When it glided for 6 seconds with a setpoint value of 6 meters, the altitude of the rocket measured by PD on the pvz3 graph was 3.974, by the second-order integral fuzzy logic on pvz2 was 6.882, by integral fuzzy logic on the pvz1 6.97, and by the fuzzy logic controller on pvz0 was 7.26. When it glided for 8 seconds with a setpoint value of 8 meters, the altitude of the rocket measured by the PD on pvz3 was 5,991, by the second-order integral fuzzy logic on pvz2 was 8.765, by integral fuzzy logic on pvz1 was 8.863, and by the fuzzy logic controller on pvz0 was 9.356.

When it glided for 10 seconds with a setpoint value of 10 meters, the altitude of the rocket measured by PD on pvz3 was 7.999, by the second-order integral fuzzy logic on pvz2 was 10.69, by integral fuzzy on pvz1 was 10.68., and by the fuzzy logic controller on pvz0 was 11.11. When it glided for 12 seconds with a setpoint value of 12 meters, the altitude of the rocket measured by PD on pvz3 was 10, by the second-order integral fuzzy on pvz2 was 12.7, by the integral fuzzy logic on pvz1 was 12.69, and by the fuzzy logic controller on pvz0 was 12.7.

When it glided for 14 seconds with a setpoint value of 14 meters, the altitude of the rocket measured by PD on the pvz3 graph was 12, by the second-order integral fuzzy on pvz2 was 14.71, by the integral fuzzy logic on pvz1 was 14.71, and by the fuzzy logic controller on pvz0 was 14.65. When it glided for 16 seconds with a setpoint value of 16 meters, the altitude of the rocket measured by PD on the pvz3 graph was 1, by the second-order integral fuzzy logic on pvz2 was 16.71, by the integral fuzzy logic is on pvz1 was 16.71, and by the fuzzy logic controller on pvz0 was 16.7.

In the first experiment, the error tracking vs time relationship graph is shown in Figure 15. From this figure, it can be seen that there are 4 graph curves, namely the ez0 graph curve shown in green, the ez1 graph curve shown in red, the ez2 graph curve. which is shown in a blue graph, and a curve of the ez3 graph which is shown in a magenta color chart.

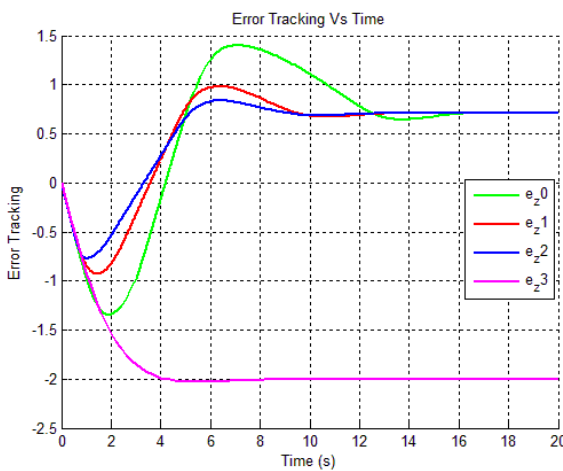


Fig. 15. Graph of the error tracking with the ramp signal time

The error tracking vs time graph in the first experiment is shown in Figure 15. The measurement result of the rocket steady state error is as follow. When the rocket glided for 2 seconds with a setpoint value of 2 meters, the steady state error value measured by PD on ez3 1.5325, by the second-order integral fuzzy logic on ez2 was 0.534, by the integral fuzzy logic on ez1 was 0.822, and by the fuzzy logic controller on pvz0 was 1.3402. When rocket glided for 4 seconds with a setpoint value of 4 meters, the steady state error value measured by PD on ez3 was 1.986, by the second-order integral fuzzy logic on ez2 was 0.279, by the integral fuzzy logic on pvz1 was 0.236, and by the fuzzy logic controller on ez0 was 0.172.

When rocket glided for 6 seconds with a setpoint value of 6 meters, the steady state error value measured by PD on ez3 was 2.026, by the second-order integral fuzzy logic on ez2 was 0.882, by the integral fuzzy logic on ez1 was 0.97, and by the fuzzy logic on ez0 was 1.26. When rocket glided for 8 seconds with a setpoint value of 8 meters, the steady state error value measured by PD on ez3 was 1.991, by the second-order integral fuzzy logic on ez2 was 0.765, by the integral fuzzy logic on ez1 was 0.861, by the fuzzy logic controller on ez0 was 1.356.

When rocket glided for 10 seconds with a setpoint value of 10 meters, the steady state error value measured by PD on ez3 was 2.001, by the second-order integral fuzzy logic on ez2 was -0.69, by the integral fuzzy logic is on ez1 was -0.68, and by the fuzzy logic controller on ez0 was -1.11. When rocket glided for 12 seconds with a setpoint value of 12 meters, the steady state error value measured by PD on the ez3 curve was 2,000, by the second-order integral fuzzy logic on ez2 was -0.7, by the integral fuzzy logic on ez1 was -0.69, and by the fuzzy logic controller on ez0 was -0.7

When rocket glided for 14 seconds with a setpoint value of 14 meters, the steady state error value measured by PD on ez3 was 2,000, by the second-order integral fuzzy logic on ez2 was -0.71, by the integral fuzzy logic on ez1 was -0.71, and by the fuzzy logic controller on ez0 was -0.65. When rocket glided for 16 seconds with a setpoint value of 16 meters, the steady state error value measured by PD on ez3 was 1.991, the second-order integral fuzzy logic on ez2 was 0.71, by integral fuzzy logic on ez1 was 0.71, and by fuzzy logic controller on ez0 was 0.7.

**B. Observation of the rocket with disturbances**

The second experiment set the rocket to track the ramp signal with a disturbance on the Z-axis, as shown in Figure 16. The Measurement result of the rocket altitude is as follow. The disturbance was given at the 10<sup>th</sup> second at the setpoint of 10 m. The setpoints of 2, 4, 6, 8 meters without disturbances generated the same result as the first experiment. Given such disturbance, the altitude value measured by PD, the second-order integral fuzzy logic the integral fuzzy logic, and the fuzzy logic controller on pvz3, pvz2, pvz1, and pvz0 when it glided:

- for 10 seconds with a setpoint value of 10 meters were 7.999, 10.71, 10.68 and 11.11, respectively.
- for 12 seconds with a setpoint value of 12 meters were 10.12.7, 12.69 and 13.78.
- for 14 seconds with a setpoint value of 14 meters were 12, 14.71, 14.71, and 14.65.
- for 16 seconds with a setpoint value of 16 meters were 14, 16.71, 16.71, and 16.7.

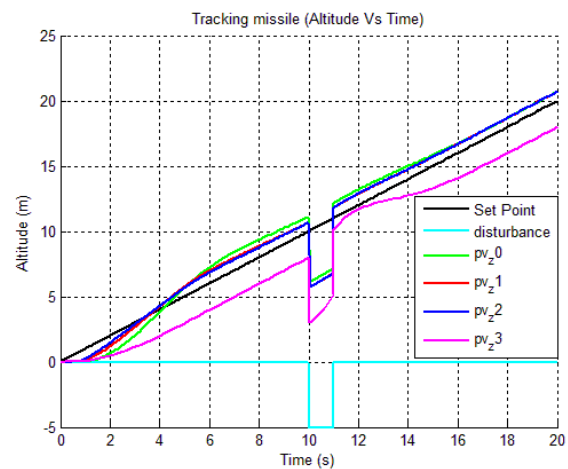


Fig. 16. Design of tracking rocket control with ramp input with disturbance

The error tracking vs time graph in the second experiment is shown in Figure 17. The measurement result of

rocket steady state error is as follow. When it glided for 2 seconds with a setpoint value of 2 meters, the steady state error value for tracking rocket control measured by PD on ez3 was 1.5325, the second-order integral fuzzy logic on ez2 was 0.534, the integral fuzzy logic on ez1 was 0.822 and the fuzzy logic controller on pvz0 was 1.3402.

- When it glided for 4 seconds with a setpoint value of 4 meters, the steady state error value for tracking rocket control measured
  - PD on ez3 was 1.986.
  - the second-order integral fuzzy logic on ez2 was 0.279.
  - the integral fuzzy logic on pvz1 graph was 0.236.
  - the fuzzy logic controller on ez0 was 0.172.
- when it glided for 6 seconds with a setpoint value of 6 meters, the steady state error value for tracking rocket control measured by
  - PD on ez3 graph was 2.026.
  - the second-order integral fuzzy on ez2 was 0.882.
  - the integral fuzzy logic on ez1 graph was 0.97.
  - the fuzzy logic controller on ez0 was 1.26.
- When it glided for 8 seconds with a setpoint value of 8 meters, the steady state error value for tracking rocket control measured by
  - PD on ez3 was 1.991.
  - the second-order integral fuzzy on ez2 graph was 0.765.
  - the integral fuzzy logic on ez1 graph was 0.861
  - the fuzzy logic controller on ez0 graph was 1.356.
- When it glided for 10 seconds with a setpoint value of 10 meters, the steady state error value for tracking rocket control measured by:
  - PD on ez3 was 2.001.
  - the second-order integral fuzzy on ez2 was 0.69.
  - integral fuzzy logic on ez1 was -0.68.
  - the fuzzy logic controller on ez0 was -1.11.
- When it glided for 12 seconds with a setpoint value of 12 meters, the steady state error value for tracking rocket control measured by
  - PD graph ez3 was -0.27
  - the second-order integral fuzzy logic on ez2 was -0.89.
  - the integral fuzzy logic on ez1 was 0.87.
  - the fuzzy logic controller on ez0 was -1.19.
- When it glided for 14 seconds with a setpoint value of 14 meters, the steady state error value for tracking rocket control measured by
  - PD graph ez3 is 1.27.
  - the second-order integral fuzzy on ez2 was -0.75.
  - using integral fuzzy logic on ez1 was -0.75.
  - using the fuzzy logic controller on was ez0.
- When it glided for 16 seconds with a setpoint value of 16 meters, the steady state error value for tracking rocket control measured by
  - the PD graph is shown in Figure ez3 at -1.89.
  - the second-order integral on ez2 was 0.69.
  - the integral fuzzy logic on ez1 was 0.69.
  - the fuzzy logic controller on ez0 as large was 0.72.

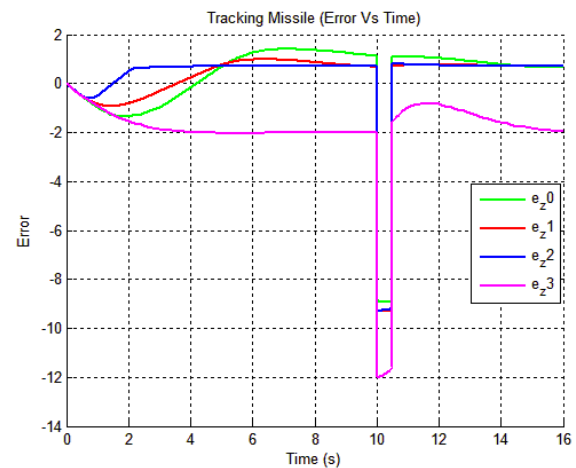


Fig. 17. Design of tracking rocket control with ramp input with disturbance

The third experiment set the rocket to track the parabolic signal without disturbances on the Z-axis, as shown in Figure 18. The measurement result of rocket altitude is as follow. The altitude value measured by PD, the second-order integral fuzzy logic, the integral fuzzy logic, and the fuzzy logic controller on pvz3, pvz2, pvz1, and pvz0 when the rocket glided:

- for 2 seconds with a setpoint value of 2.982 meters were 5716, 2.982, 0.5716, and 0.5716, respectively.
- for 4 seconds with a setpoint value of 15.47 meters were 5.29, 15.47, 2.833, and 2.833, respectively.
- for 6 seconds with a setpoint value of 35.7 meters were 17.27, 35.7, 5.233, and 5.233, respectively.
- for 8 seconds with a setpoint value of 62.91 meters were 37.22, 99.97, using integral fuzzy logic on pvz1 was 8.863, 9.356, respectively.
- for 10 seconds with a setpoint value of 99.97 meters were 65.21, 99.97, was 10.03, and 10.03, respectively.
- for 12 seconds with a setpoint value of 143.1 meters were 101.2, 143.1, 12.43, and 12.43, respectively.
- for 14 seconds with a setpoint value of 195.2 meters were 145.2, 195.2, 14.83, and 14.83, respectively.
- for 16 seconds with a setpoint value of 255.9 meters were 197.2, 255.9, 17.23, and 17.23, respectively.

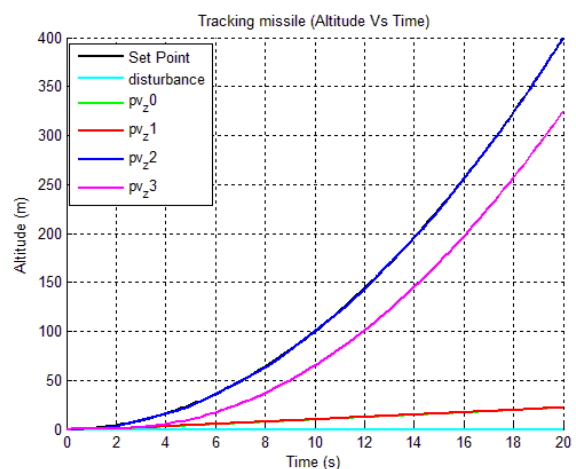


Fig. 18. Tracking rocket with parabolic input without disturbance

The error tracking vs time graph in the third experiment is shown in Figure 19. The measurement result of the rocket steady state error is as follow. When it glided for 2 seconds with a setpoint value of 2.982 meters, the steady state error value measured by PD on ez3 graph was 2.4104, by the second-order integral fuzzy logic on ez2 was 0, by the integral fuzzy logic on ez1 was 2.411, and by the fuzzy logic controller on pvz0 was 2.411. When it glided for 4 seconds with a setpoint value of 15.47 meters, the steady state error value measured by PD on ez3 graph was 10.18, by the second-order integral fuzzy logic on ez2 was 0, by the integral fuzzy logic on ez1 was 12.637, and by the fuzzy logic controller on pvz0 was 12.637.

When it glided for 6 seconds with a setpoint value of 35.7 meters, the steady state error value measured by PD on ez3 was 18.43, by the second-order integral fuzzy logic on ez2 was 0, by the integral fuzzy logic on ez1 was 30.467, and by the fuzzy logic controller on pvz0 was 30.467. When it glided for 8 seconds with a setpoint value of 62.91 meters, the steady state error value measured by PD on ez3 was 25.69, by the second-order integral fuzzy logic on ez2 was 0, by the integral fuzzy logic on ez1 was 55.277., and by the fuzzy logic controller on pvz0 was 12.637, 55.277.

when it glided for 10 seconds with a setpoint value of 99.97 meters, the steady state error value measured by PD on ez3 was 34.76, by the second-order integral fuzzy logic on ez2 was 0, by the integral fuzzy logic on ez1 was 89.94., and by the fuzzy logic controller on pvz0 was 89.94. When it glided for 12 seconds with a setpoint value of 143.1 meters, the steady state error value measured by PD on ez3 was 41.9, by the second-order integral fuzzy logic on ez2 was 0, by the integral fuzzy logic on ez1 was 130.67., and by the fuzzy logic controller on pvz0 was 130.67.

When it glided for 14 seconds with a setpoint value of 195.2 meters, the steady state error value measured by PD on ez3 was 50, by the second-order integral fuzzy logic on ez2 was 0, by the integral fuzzy logic on ez1 was 180.37., and by the fuzzy logic controller on pvz0 was 180.37. When it glided for 16 seconds with a setpoint value of 255.9 meters, the steady state error value measured by PD on ez3 was 58.7, by the second-order integral fuzzy logic on ez2 was 0, by the integral fuzzy logic on ez1 was 255.9, and by the fuzzy logic controller on pvz0 was 255.9.

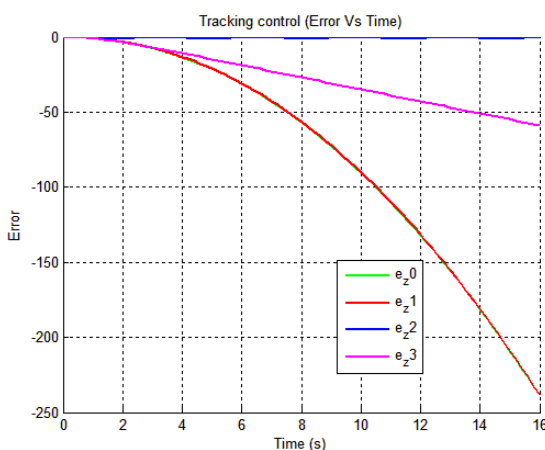


Fig. 19. Graph of the error relationship to the time of the ramp signal

The fourth experiment set the rocket to track the parabolic signal with wind disturbances on the Z-axis, as shown in Figure 20. The measurement result of the rocket altitude is as follow. The altitude value measured by PD, the second-order integral fuzzy logic, the integral fuzzy logic, and the fuzzy logic controller on pvz3, pvz2, pvz1, and pvz0 when the rocket glided,

- for 2 seconds with a setpoint value of 2.982 meters were 0.5716, 2.982, 0.5716, and 0.5716, respectively.
- for 4 seconds with a setpoint value of 15.47 meters were 5.29, 15.47, 2.833, and 2.833, respectively
- for 6 seconds with a setpoint value of 35.7 meters were 17.27, 35.7, 5.233, and 5.233, respectively.
- for 8 seconds with a setpoint value of 62.91 meters were 37.22, 99.97, 8.863, 9.356, respectively.
- for 10 seconds with a setpoint value of 99.97 meters were 65.21, 99.97, 10.03, and 10.03, respectively.
- for 12 seconds with a setpoint value of 143.1 meters were 101.2, 143.1, 12.43, and 12.43, respectively.
- for 14 seconds with a setpoint value of 195.2 meters were 145.2, 195.2, 14.83, and 14.83, respectively.
- for 16 seconds with a setpoint value of 255.9 meters were 197.2, 255.9, 17.23, and 17.23, respectively.

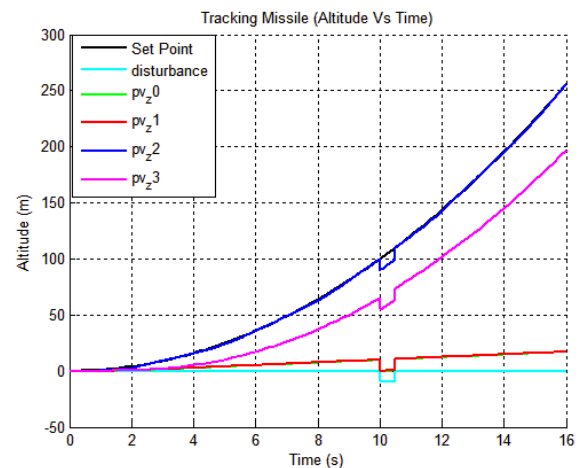


Fig. 20. Rocket tracking control design with ramp input with disturbance

The error tracking vs time graph in the fourth experiment is shown in Figure 21. There are four curves, namely the ez0 curve shown in green, the ez1 curve in red, the ez2 curve in blue, and ez3 curve in a magenta. The measurement result of the rocket steady state error is as follow. When it glided for 2 seconds with a setpoint value of 2.982 meters, the steady state error value measured by PD on ez3 graph was 2.4104, by the second-order integral fuzzy logic on ez2 was 0, by the integral fuzzy logic on ez1 was 2.411, and by the fuzzy logic controller on pvz0 was 2.411. When it glided for 4 seconds with a setpoint value of 15.47 meters, the steady state error value measured by PD on ez3 graph was 10.18, by the second-order integral fuzzy logic on ez2 was 0, by the integral fuzzy logic on ez1 was 12.637, and by the fuzzy logic controller on pvz0 was 12.637.

When it glided for 6 seconds with a setpoint value of 35.7 meters, the steady state error value measured by PD on ez3 was 18.43, by the second-order integral fuzzy logic on ez2 was 0, by the integral fuzzy logic on ez1 was 30.467, and by

the fuzzy logic controller on pvz0 was 30.467. When it glided for 8 seconds with a setpoint value of 62.91 meters, the steady state error value measured by PD on ez3 was 25.69, by the second-order integral fuzzy logic on ez2 was 0, by the integral fuzzy logic on ez1 was 55.277., and by the fuzzy logic controller on pvz0 was 12.637, 55.277.

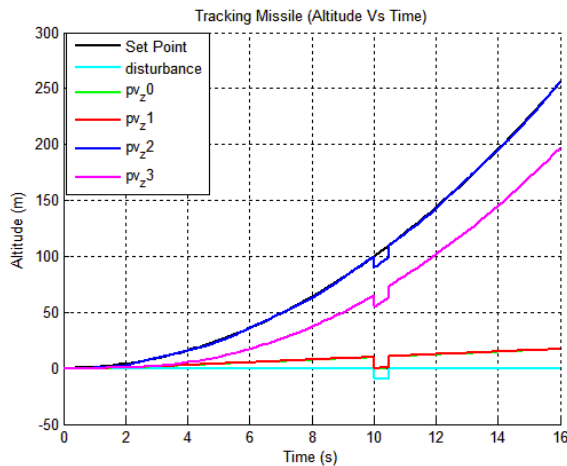


Fig. 21. The graph of the error relationship to the time of the ramp signal with the disturbance.

when it glided for 10 seconds with a setpoint value of 99.97 meters, the steady state error value measured by PD on ez3 was 34.76, by the second-order integral fuzzy logic on ez2 was 0, by the integral fuzzy logic on ez1 was 89.94., and by the fuzzy logic controller on pvz0 was 89.94. When it glided for 12 seconds with a setpoint value of 143.1 meters, the steady state error value measured by PD on ez3 was 41.9, by the second-order integral fuzzy logic on ez2 was 0, by the integral fuzzy logic on ez1 was 130.67., and by the fuzzy logic controller on pvz0 was 130.67.

When it glided for 14 seconds with a setpoint value of 195.2 meters, the steady state error value measured by PD on ez3 was 50, by the second-order integral fuzzy logic on ez2 was 0, by the integral fuzzy logic on ez1 was 180.37., and by the fuzzy logic controller on pvz0 was 180.37. When it glided for 16 seconds with a setpoint value of 255.9 meters, the steady state error value measured by PD on ez3 was 58.7, by the second-order integral fuzzy logic on ez2 was 0, by the integral fuzzy logic on ez1 was 255.9, and by the fuzzy logic controller on pvz0 was 255.9.

## V. CONCLUSION

The paper described the latest developments in rocket tracking control. There are four tracking rocket controls tested both with and without disturbances with ramp and parabolic inputs using a fuzzy logic algorithm by combining proportional control so that the rocket can glide according to the parabolic and ramp trajectories. The proposed algorithm shows that the rocket glides 12.78m at 12 seconds with a steady-state error of 0.78 according to the ramp path setpoint 12 m; 10.68m at 10 seconds with a steady-state error of 0.68 according to the ramp path setpoint 10m; and 4.689m at 4 seconds with a steady-state error of 0.689 according to the ramp path setpoint 4m. In accordance with the parabolic path,

the rocket glides 15.47m at the 4th minute with 0 steady-state error.

## REFERENCES

- [1] G. Chen, Z. Li, Z. Zhang, and S. Li, "An Improved ACO Algorithm Optimized Fuzzy PID Controller for Load Frequency Control in Multi Area Interconnected Power Systems," *IEEE Access*, vol. 8, pp. 6429–6447, 2020.
- [2] Z. Yan, Z. Yang, J. Zhang, J. Zhou, A. Jiang, and X. Du, "Trajectory Tracking Control of UAV Based on Backstepping Sliding Mode With Fuzzy Switching Gain in Diving Plane," *IEEE Access*, vol. 7, pp. 166788–166795, 2019.
- [3] N. P. Nguyen, H. Oh, Y. Kim, J. Moon, J. Yang, and W.-H. Chen, "Fuzzy-Based Super-Twisting Sliding Mode Stabilization Control for Under-Actuated Rotary Inverted Pendulum Systems," *IEEE Access*, vol. 8, pp. 185079–185092, 5393.
- [4] S. Hou, J. Fei, Y. Chu, and C. Chen, "Experimental Investigation of Adaptive Fuzzy Global Sliding Mode Control of Single-Phase Shunt Active Power Filters," *IEEE Access*, vol. 7, pp. 64442–64449, 2019.
- [5] J. Gamiz, R. Vilanova, H. Martinez-Garcia, Y. Bolea, and A. Grau, "Fuzzy Gain Scheduling and Feed-Forward Control for Drinking Water Treatment Plants (DWTP) Chlorination Process," *IEEE Access*, vol. 8, pp. 110018–110032, 2020.
- [6] F. You, N. Chen, Z. Zhu, S. Cheng, H. Yang, and M. Jia, "Adaptive Fuzzy Control for Nonlinear State Constrained Systems With Input Delay and Unknown Control Coefficients," *IEEE Access*, vol. 7, pp. 53718–53730, 2019.
- [7] X. Tang, D. Ning, H. Du, W. Li, Y. Gao, and W. Wen, "A Takagi-Sugeno Fuzzy Model-Based Control Strategy for Variable Stiffness and Variable Damping Suspension," *IEEE Access*, vol. 8, pp. 71628–71641, 2020.
- [8] J. Yang et al., "EKF Based Fuzzy PI Controlled Speed Sensorless Power Optimal Control of a Direct Drive Power System," *IEEE Access*, vol. 7, pp. 61610–61619, 2019.
- [9] E. D. S. Oliveira, R. H. C. Takahashi, and W. M. Caminhas, "Online Neuro-Fuzzy Controller: Design for Robust Stability," *IEEE Access*, vol. 8, pp. 193768–193776, 2020.
- [10] H. K. Tran, J.-S. Chiou, N. T. Nam, and V. Tuyen, "Adaptive Fuzzy Control Method for a Single Tilt Tricopter," *IEEE Access*, vol. 7, pp. 161741–161747, 2019.
- [11] Y. Huang, T. Wang, J. Wang, K. Ma, C. Zhang, and X. Huang, "Extended Fuzzy Adaptive Event-Triggered Compensation Control for Uncertain Nonlinear Systems With Input Hysteresis," *IEEE Access*, vol. 7, pp. 89658–89669, 2019.
- [12] Y. Liu, P. Yang, L. Cao, Y. Li, R. Wang, and X. Sun, "High Order Sliding Mode Backstepping Control for a Class of Unknown Pure Feedback Nonlinear Systems," *IEEE Access*, vol. 8, pp. 227528–227537, 2020.
- [13] X. Fan, Y. He, P. Cheng, and M. Fang, "Fuzzy-Type Fast Terminal Sliding-Mode Controller for Pressure Control of Pilot Solenoid Valve in Automatic Transmission," *IEEE Access*, vol. 7, pp. 122342–122353, 2019.
- [14] H. Hu, X. Wang, and L. Chen, "Impedance Sliding Mode Control With Adaptive Fuzzy Compensation for Robot-Environment Interacting," *IEEE Access*, vol. 8, pp. 19880–19889, 2020.
- [15] X. Bu, "Actor-Critic Reinforcement Learning Control of Non-Strict Feedback Nonaffine Dynamic Systems," *IEEE Access*, vol. 7, pp. 65569–65578, 5292.
- [16] T. Sadeq, C. K. Wai, E. Morris, Q. A. Tarboosh, and O. Aydogdu, "Optimal Control Strategy to Maximize the Performance of Hybrid Energy Storage System for Electric Vehicle Considering Topography Information," *IEEE Access*, vol. 8, pp. 216994–217007, 2020.
- [17] H. Rezk, M. Aly, M. Al-Dhaifallah, and M. Shoyama, "Design and Hardware Implementation of New Adaptive Fuzzy Logic-Based MPPT Control Method for Photovoltaic Applications," *IEEE Access*, vol. 7, pp. 106427–106438, 2019.
- [18] D. Liu, S. Zhao, and X. Luo, "Adaptive Fuzzy Control for the Generalized Projective Synchronization of Fractional-Order

- Extended Hindmarsh-Rose Neurons,” *IEEE Access*, vol. 8, pp. 190689–190699, 2020.
- [19] H. Xue, Z. Zhang, M. Wu, and P. Chen, “Fuzzy Controller for Autonomous Vehicle Based on Rough Sets,” *IEEE Access*, vol. 7, pp. 147350–147361, 2019.
- [20] H. Wu, H. An, Q. Wei, and H. Ma, “Fuzzy CMAC-Based Adaptive Scale Force Control of Body Weight Support Exoskeletons,” *IEEE Access*, vol. 8, pp. 147286–147294, 2020.
- [21] M. Rabah, A. Rohan, S. A. S. Mohamed, and S.-H. Kim, “Autonomous Moving Target-Tracking for a UAV Quadcopter Based on Fuzzy-PI,” *IEEE Access*, vol. 7, pp. 38407–38419, 2019.
- [22] Y. Guo and M. E. A. Mohamed, “Speed Control of Direct Current Motor Using ANFIS Based Hybrid P-I-D Configuration Controller,” *IEEE Access*, vol. 8, pp. 125638–125647, 2020.
- [23] C. Bao, H. Guo, L. Kong, and X. Cheng, “Multi-Stage Gear Shifting Control Scheme for Electric Mechanical Transmission: Design and Experiment,” *IEEE Access*, vol. 7, pp. 95576–95584, 2019.
- [24] Y. Chen, Q. Gao, J. Cheng, K. Shi, and W. Qi, “Static Output Feedback Control for Fuzzy Systems With Stochastic Fading Channel and Actuator Faults,” *IEEE Access*, vol. 8, pp. 200714–200723, 2020.
- [25] W. Kang, S. Li, and D.-W. Ding, “Input-to-State Stabilization of Uncertain Parabolic PDEs Using an Observer-Based Fuzzy Control,” *IEEE Access*, vol. 7, pp. 3581–3591, 2019.
- [26] Z. Liu, P. Zhang, K. Y. Chan, K. Ma, and L. Li, “Robust Power Allocation for Femtocell Networks Using Fuzzy Estimation of Dynamic Channel States,” *IEEE Access*, vol. 7, pp. 22872–22883, 2019.
- [27] X. Liu, S. Zhen, H. Zhao, H. Sun, and Y.-H. Chen, “Fuzzy-Set Theory Based Optimal Robust Design for Position Tracking Control of Permanent Magnet Linear Motor,” *IEEE Access*, vol. 7, pp. 153829–153841, 2019.
- [28] J. Wu, M. Dong, K. Ota, M. Tariq, and L. Guo, “Cross-Domain Fine-Grained Data Usage Control Service for Industrial Wireless Sensor Networks,” *IEEE Access*, vol. 3, pp. 2939–2949, 2015.
- [29] H. ZHAO, Q. WU, C. WANG, L. CHENG, and C. N. RASMUSSEN, “Fuzzy logic based coordinated control of battery energy storage system and dispatchable distributed generation for microgrid,” *J. Mod. Power Syst. Clean Energy*, vol. 3, no. 3, pp. 422–428, Sep. 2015.
- [30] P.-H. Kuo, T.-H. S. Li, Y.-F. Ho, and C.-J. Lin, “Development of an Automatic Emotional Music Accompaniment System by Fuzzy Logic and Adaptive Partition Evolutionary Genetic Algorithm,” *IEEE Access*, vol. 3, pp. 815–824, 2015.
- [31] R. Mahony, V. Kumar, and P. Corke, “Multirotor Aerial Vehicles: Modeling, Estimation, and Control of Quadrotor,” *IEEE Robot. Autom. Mag.*, vol. 19, no. 3, pp. 20–32, Sep. 2012.
- [32] Iswanto, O. Wahyunggoro, and A. I. Cahyadi, “Hover position of quadrotor based on PD-like fuzzy linear programming,” *Int. J. Electr. Comput. Eng.*, vol. 6, no. 5, pp. 2251–2261, 2016.